行政院國家科學委員會補助專題研究計畫成果報告

※※※※※※※※※※※※※※※※※※※※※※※※※
※ ※
※ 在異質狀態下、可壓縮流問題的 ※
※ 有效解法（3/3） ※
※ ※
※※※※※※※※※※※※※※※※※※※※※※※※※

計畫類別：☑個別型計畫 □整合型計畫

計畫編號：NSC90－2115－M－002－022

執行期間：90 年 08 月 01 日至 91 年 07 月 31 日

計畫主持人：薛克民

共同主持人：

本成果報告包括以下應繳交之附件：

□赴國外出差或研習心得報告一份

□赴大陸地區出差或研習心得報告一份

□出席國際學術會議心得報告及發表之論文各一份

□國際合作研究計畫國外研究報告書一份

執行單位：台大數學系

中 華 民 國 91 年 12 月 30 日

Multifluid Computations with Vacuum and Elastic-Plastic Conditions: One-Dimensional Case *

Keh-Ming Shyue †

December 30, 2002

This brief note describes the recent progress of our development to an efficient multicomponent algorithm for elastic-plastic flow in solids. As a first attempt to model the flow, we use a mathematical formulation given by Wilkins [8] in that the equations of motion, in one dimension, takes the form

$$\frac{\partial}{\partial t}\begin{pmatrix}\rho\\ \rho u\\ \rho E\end{pmatrix}+\frac{\partial}{\partial x}\begin{pmatrix}\rho u\\ \rho u^2-\sigma_x\\ \rho E u-\sigma_x u\end{pmatrix}=0,$$

where ρ denotes the density, u is the particle velocity, $\sigma_x = -p + s_x$ is the total stress, and $E = e + u^2/2$ is the specific total energy. Here depending on the physical domain of interests, the hydrostatic pressure p is assumed to be either a function of the density only or a function of both the density and the specific internal energy e (see below for an example). We consider the Hookes' law for the constitutive relation between the stress and strain rate, and so have the stress deviator s_x governed by the following equation

$$\frac{Ds_x}{Dt}=2\mu\left(\frac{D\epsilon_x}{Dt}+\frac{1}{3\rho}\frac{D\rho}{Dt}\right).$$

Note that μ denotes the shear modulus, $D\epsilon_x/Dt$ is the strain rate deviator, and $D(\cdot)/Dt$ means the time derivative of a quantity along a particle path. To complete the model, the von Mises yield condition is used to describe the elastic limit, and in one dimension this is that

$$s_x^2\le\frac{2}{3}Y_0^2,$$

where Y_0 is the yield strength of the material (cf. [8] for the more details). It should be mentioned that when this inequality is violated, plastic flow begins to occur, and for perfectly-plastic flow the stress deviator is assumed to remain constant beyond this point, see Fig. 1 for a typical loading and unloading paths for an elastic-plastic (perfectly) flow in solids.

We are interested in a class of elastic-plastic flow problems with fracture or cavitation. Consider a popular flying aluminum-plate problem of Wilkins [8], for example. We use the polynomial equation of state of the form

$$p(\rho)=A\left(\rho/\rho_0-1\right)+B\left(\rho/\rho_0-1\right)^2+C\left(\rho/\rho_0-1\right)^3$$

*The final report for NSC project: Efficient Solution Methods for Compressible Flow Problems in Heterogeneous Media (3/3) (Grant number: NSC 90-2115-M-002-022)

†Department of Mathematics, National Taiwan University, Taipei, Taiwan, 106, Republic of China (shyue@math.ntu.edu.tw).

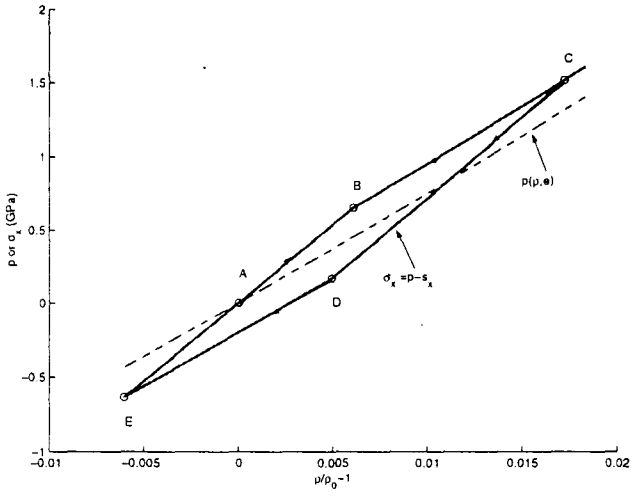

Figure 1: A typical loading ($A \to B \to C$) and unloading ($C \to D \to E$) paths for an elastic-plastic (perfectly) flow in solids without the work hardening effect.

with $\rho_0 = 2.7$ Mg/m^3, $A = 73$GPa, $B = 172$GPa, and $C = 40$GPa, to model the hydrostatic pressure of the aluminum, and take $\mu = 24.8$GPa and $Y_0 = 0.2976$GPa in our elastic-plastic model for the possible resistance of the material to shear distortion. As for the initial condition, we take

$$(\rho,\ u) = \begin{cases} \text{vacuum} & \text{for } x < 1\text{mm} \\ (\rho_0,\ u_0) & \text{for } 1\text{mm} \le x < 5\text{mm} \\ (\rho_0,\ 0) & \text{for } 5\text{mm} \le x \le 50\text{mm} \end{cases}$$

with u_0 denoted the initial impact velocity of the moving aluminum plate.

We run this problem using a high-resolution front-tracking method with a HLL-type approximate Riemann solver [7], the MINMOD limiter [1], the Courant number 0.9, and the mesh size $\Delta x = 1/10$mm. Results for the elastic-plastic flow calculations with $u_0 = 0.8$km/s and 2km/s are shown in Figs. 2 and 3, respectively. In the case of 0.8km/s (see Fig. 2), we observe a plastic shock wave trailing behind an elastic shock precursor, while in the case of 2km/s (see Fig. 3), since the shock stress-deviator is above the elastic limit, we only see the plastic shock. In both cases, when the leftward-going shock waves reach the free surface, a leading rightward-going elastic rarefaction is formed, followed by the plastic rarefaction wave. As the time goes on, these waves begin to overtake the initial rightward-going shocks. It is easy to check that these results are in good agreement with Wilkins' [8] and Miller-Colella's [3].

To see the effect of the elastic-plastic condition to the basic structure of the solution, Figs. 4 and 5 show numerical results without the elastic-plastic condition. Clearly, now all the waves are hydrodynamic waves, and so there is no precursor elastic wave (shock or rarefaction) occurring in the solution (cf. [4] for a similar calculation but with the full Euler equation and a Mie-Grüneisen equation of state). It should be mentioned that in this problem the free-surface boundary is tracked and evolved according to a speed of the vacuum boundary determined by the vacuum Riemann problem (cf. [7]).

We are next concerned with a model problem with spall. Motivated by a hydrodynamic calculation of Miller and Puckett [4], we consider the simulation of the collision of two rarefaction waves in a precompressed aluminum plate within a vacuum that incorporates plasticity. In this case, the

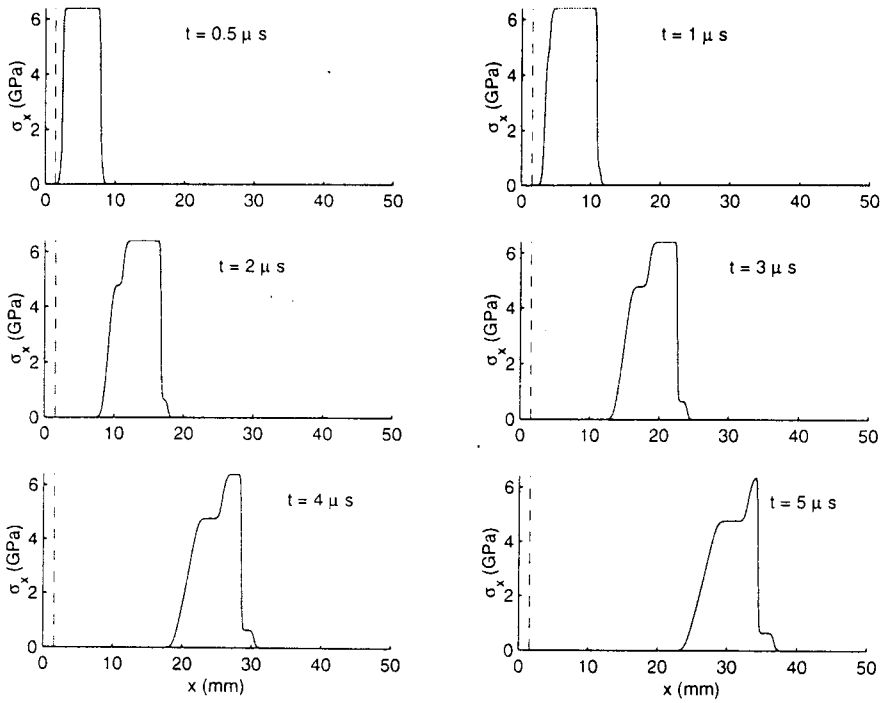

Figure 2: Elastic-plastic flow calculations for Wilkins' problem with impact velocity 0.8km/s. Total stress σ_x is shown at six different times $t = 0.5$, 1, 2, 3, 4, and 5μs. The dashed line in each subplot is the approximate location of the free surface.

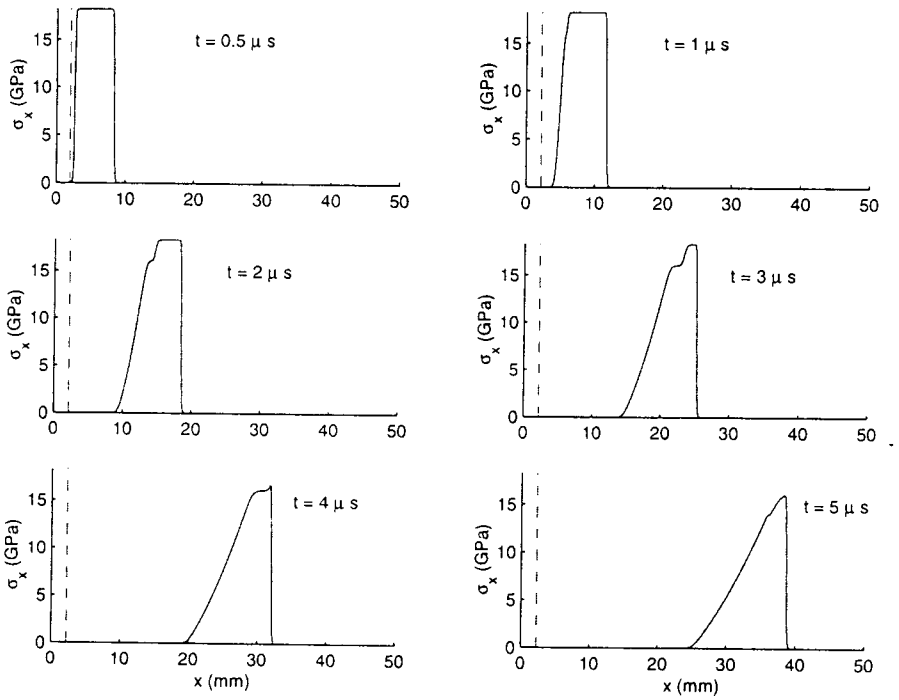

Figure 3: Elastic-plastic flow calculations for Wilkins' problem with impact velocity 2km/s. The graphs of the solutions are displayed in the same manner as in Fig. 2.

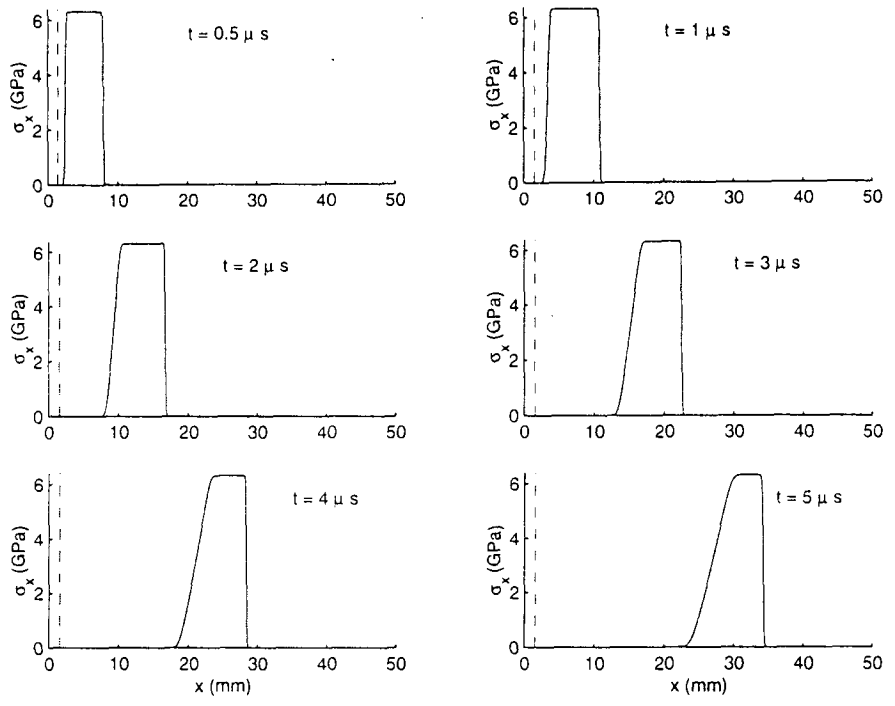

Figure 4: Hydrodynamic flow calculations for Wilkins' problem with impact velocity 0.8km/s. The graphs of the solutions are displayed in the same manner as in Fig. 2.

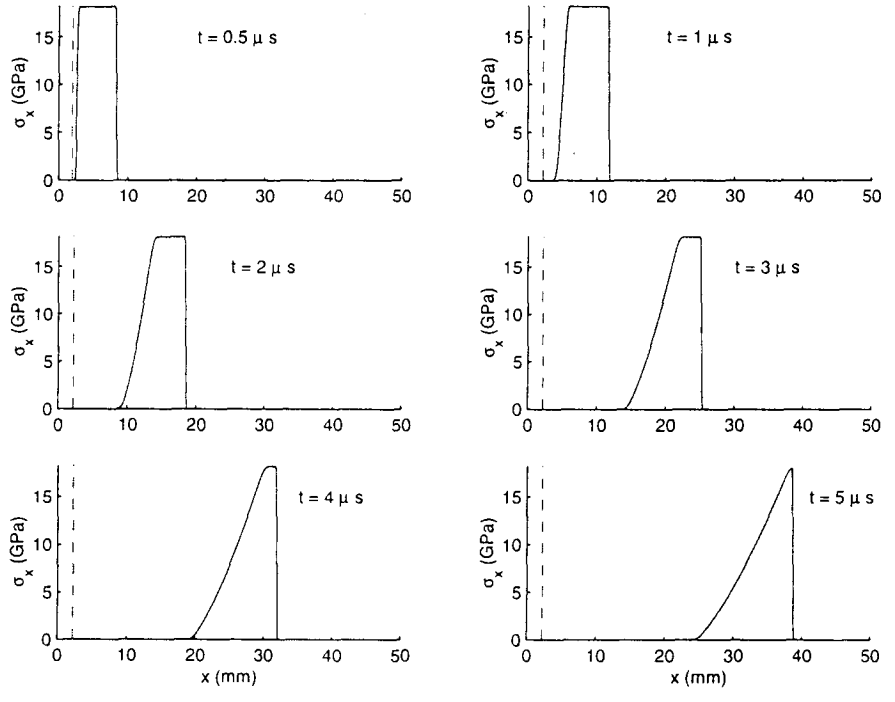

Figure 5: Hydrodynamic flow calculations for Wilkins' problem with impact velocity 2km/s. The graphs of the solutions are displayed in the same manner as in Fig. 2.

initial condition we take is

$$(\rho,\ u,\ p) = \begin{cases} \text{vacuum} & \text{for } x < 10\text{mm} \\ (2785\text{kg/m}^3,\ 0,\ 13\text{GPa}) & \text{for } 10\text{mm} \le x < 40\text{mm}, \\ \text{vacuum} & \text{for } 40\text{mm} \le x \le 50\text{mm}, \end{cases}$$

and the equation of state for the hydrostatic pressure of aluminum is

$$p = \begin{cases} p_{\text{ref}}(\rho) + \Gamma(\rho)\rho\left[e - e_{\text{ref}}(\rho)\right] & \text{for } \rho \ge \rho_0 \\ A\,(\rho/\rho_0)^{\alpha} - B & \text{for } \rho < \rho_0. \end{cases}$$

Here written in terms of the specific volume $V = 1/\rho$, the function Γ, p_{ref}, and e_{ref} take the form:

$$\Gamma(V) = \Gamma_0 \left(\frac{V}{V_0}\right)^q, \quad p_{\text{ref}}(V) = p_0 + \frac{c_0^2(V_0 - V)}{[V_0 - s(V_0 - V)]^2}, \quad e_{\text{ref}}(V) = e_0 + \frac{1}{2}\left[p_{\text{ref}}(V) + p_0\right](V_0 - V),$$

and $A = p_0 + K_{0S}/K'_{0S}$, $B = K_{0S}/K'_{0S}$, and $\alpha = K'_{0S}$ with $K_{0S} = \rho_0 c_0^2$ and $K'_{0S} = 4s - 1$ (cf. [5]). Note that c_0 denotes the zero-pressure isentropic speed of sound, and q and s are dimensionless parameters.

We carried out the computation using the same numerical method as before, and dsplayed the results in Figs. 6 and 7 for the density, velocity, total stress, and the vacuum fraction at four different times $t = 1$, 2, 3, and 10μs. It is clear that the passage of the initial leftward- and rightward-going rarefaction waves through the material creates tension when they collide, and vacuum is introduced when the total stress σ_x drops below the critical value $\sigma_v = -2$GPa.

To end this note, we mention that a more detailed description of the method along with some additional results can be found in [6]. In the future, we plan to extend the method to two-dimensional elastic-plastic in solids, and consider more realistic constitutive model for a rate-dependent stress-strain relationship.

References

[1] R. J. LeVeque and K.-M. Shyue. One-dimensional front tracking based on high resolution wave propagation methods. *SIAM J. Sci. Comput.*, 16:348–377, 1995.

[2] R. Menikoff and B. Plohr. The Riemann problem for fluid flow of real materials. *Rev. Mod. Phys.*, 61:75–130, 1989.

[3] G. H. Miller and P. Colella. A high-order Eulerian Godunov method for elastic-plastic flow in solids. *J. Comput. Phys.*, 167:131–176, 2001.

[4] G. H. Miller and E. G. Puckett. A high order Godunov method for multiple condensed phases. *J. Comput. Phys.*, 128:134–164, 1996.

[5] A. L. Ruoff. Linear shock-velocity-particle-velocity relationship. *J. Appl. Phys.*, 38(13):4976–4980, 1967.

[6] K.-M. Shyue. A simple volume tracking method for compressible flow with vacuum. *submitted for publication*, 2002.

[7] K.-M. Shyue. A wave propagation method for elastic-plastic flow in solids: One-dimensional case. *submitted for publication*, 2002.

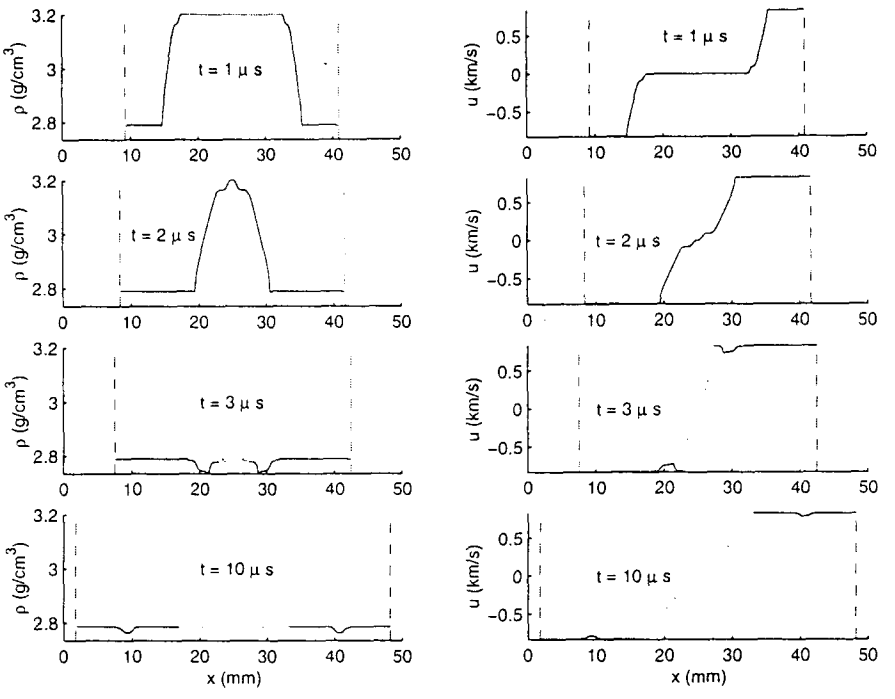

Figure 6: Elastic-plastic flow calculations for a model spall problem. Density ρ and velocity u are shown on the left and right column, respectively, at four different times $t = 1$, 2, 3, and 10μs. The dashed lines in each subplot are the approximate location of the free surface.

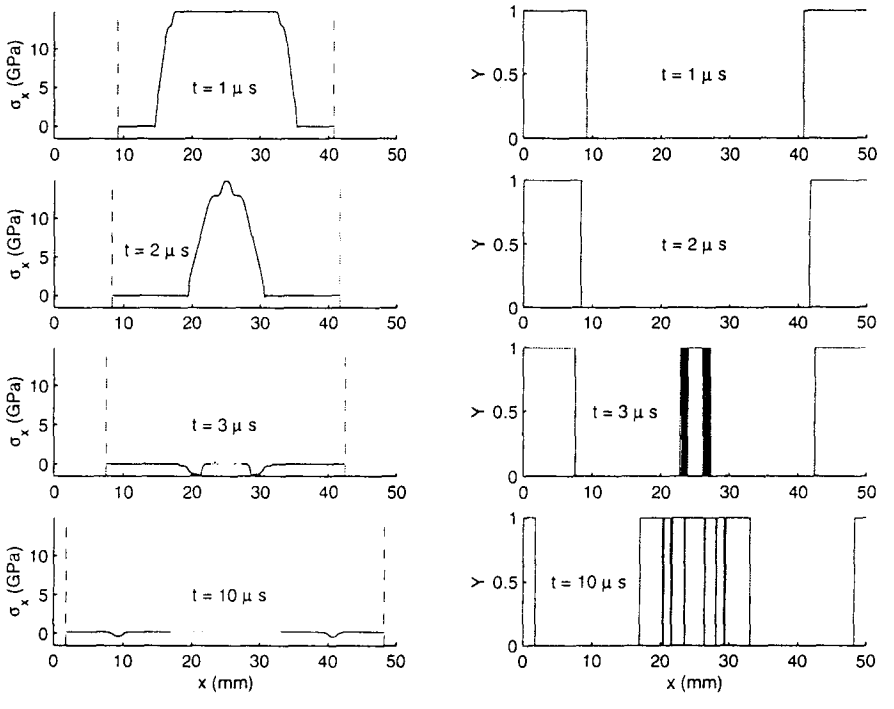

Figure 7: Elastic-plastic flow calculations for a model spall problem. Total stress σ_x and vacuum fraction Y are shown on the left and right column, respectively, at four different times $t = 1$, 2, 3, and 10μs.

[8] M. L. Wilkins. Calculation of elastic-plastic flow. In B. Adler, S. Fembach, and M. Rotenberg, editors, *Methods in Computational Physics, Vol. 3*, pages 211–263. Academic Press, New York, 1964.

[9] M. L. Wilkins. *Computer Simulation of Dynamic Phenomena.* Springer, New York, 1999.